Acta Crystallographica Section A
Foundations and Advances
ISSN 2053-2733

Received 11 October 2013
Accepted 6 November 2013

Darwin's approach to X-ray diffraction on lateral crystalline structures

Vasily I. Punegov,[a]* Sergey I. Kolosov[a] and Konstantin M. Pavlov[b,c]

[a]Komi Research Center, Ural Division, Russian Academy of Sciences, 167982, Syktyvkar, Russian Federation, [b]School of Science and Technology, University of New England, NSW 2351, Australia, and [c]School of Physics, Monash University, VIC 3800, Australia. Correspondence e-mail: vpunegov@dm.komisc.ru

Darwin's dynamical theory of X-ray diffraction is extended to the case of lateral (*i.e.*, having a finite length in the lateral direction) crystalline structures. This approach allows one to calculate rocking curves as well as reciprocal-space maps for lateral crystalline structures having a rectangular cross section. Numerical modelling is performed for these structures with different lateral sizes. It is shown that the kinematical approximation is valid for thick crystalline structures having a small length in the lateral direction.

1. Introduction

There are several approaches to X-ray dynamical diffraction by crystals (see, *e.g.*, Authier, 2001; Pietsch *et al.*, 2004 and references therein). Among them Darwin's diffraction theory (Darwin, 1914*a*,*b*), based on recurrence relations, presents arguably the most simple and transparent way to describe X-ray and neutron dynamical diffraction by crystals. However, Darwin's theory (in its original formulation) has more restrictions in comparison with Laue–Ewald's theory (see, *e.g.*, Authier, 2001); therefore it was not widely used. Borie (1966) first used Darwin's recurrence relations to describe the Borrmann effect. Using Borie's approach, Bezirganian & Navasardian (1969) showed that the Borrmann effect depends on the lateral size of crystals. Darwin's theory was also used to investigate (i) diffraction in the asymmetric Laue geometry (Borie, 1967; Kuznetsov & Fofanov, 1970), (ii) multiwave diffraction (Kuznetsov & Fofanov, 1972; Ignatovich, 1992) and (iii) properties of the dispersion surface (Borie, 1967). The recurrence relations for the amplitudes of transmitted and reflected waves were also employed to investigate neutron diffraction by polyatomic crystals (Ignatovich, 1990) and scattering of visible light in liquid crystals (Chandrasekhar & Rao, 1968). Darwin's recurrence relations were also used in multilayer materials optics (Dub & Litzman, 1999).

The crystal truncation rod (CTR) method (Robinson, 1986) was originally developed within the framework of kinematical diffraction for characterization of surface layers. Darwin's dynamical diffraction approach was implemented in the CTR technique in Caticha (1994), Nakatani & Takahashi (1994), Takahashi & Nakatani (1995), Durbin & Follis (1995) and Takahashi *et al.* (2000).

Yashiro & Takahashi (2000) analysed the reflection and transmission coefficients of a single atomic plane for an arbitrary two-dimensional Bravais lattice. Their results (Yashiro & Takahashi, 2000) are similar to those obtained by Borie (1967); however, they differ from ones obtained by Durbin (1995). Later, on the basis of Yashiro & Takahashi (2000) a variant of Darwin's theory for grazing-incidence geometry was developed (Yashiro *et al.*, 2001).

Prins (1930) analysed the effects of refraction and absorption for semi-infinite crystals. An exact solution of Darwin's recurrence equations for a crystal with an arbitrary number of reflecting planes was obtained by Perkins & Knight (1984) with the use of the Chebyshev polynomials (Abramowitz & Stegun, 1972). Chen & Bhattacharya (1993) showed that the Darwin recurrence relations are identical to Takagi's differential equations (Takagi, 1962) as one goes from an array of discrete atomic planes to a continual model of medium.

Most crystalline structures are non-ideal, *e.g.*, they contain defects. Statistical dynamical diffraction theory (in the case of a plane-wave illumination) (Bushuev, 1989; Punegov, 1990, 1991, 1993; Pavlov & Punegov, 1998, 2000) using Takagi's equations (Takagi, 1962) is one possible way to describe X-ray dynamical diffraction in such structures. However, Darwin's theory (Darwin, 1914*a*,*b*), which was originally developed for an ideal crystal, can also be modified for use with non-ideal crystals. For instance, Chung & Durbin (1999) considered the thermal vibration effect. Li *et al.* (1997) examined the influence of statistically distributed defects. X-ray diffraction is particularly sensitive to deformation of the crystalline lattice, which is another variant of deviations from an ideal crystalline structure. First attempts at modelling X-ray diffraction by a crystal with a linear lattice parameter variation using Darwin's approach were done by Fitzgerald & Darlington (1976). Their numerical results were confirmed later by analytical solutions (Kolpakov & Punegov, 1985; Punegov & Vishnjakov, 1995). Prudnikov obtained analytical solutions for the cases of crystals distorted by surface acoustic waves (Prudnikov, 1998) and non-ideal heterostructures (Prudnikov, 2000).

Recurrence relations (similar to Darwin's equations) were obtained for multilayer structures. Therewith the reflection

and transmission coefficients for a single atomic plane were replaced by the appropriate coefficients for crystalline layers (Belyaev & Kolpakov, 1983; Bartels *et al.*, 1986). This approach was further extended to multiwave diffraction (Ladanov & Punegov, 1989; Punegov, 1993), highly asymmetrical diffraction geometry (Punegov & Ladanov, 1989*b*, 1990) and glancing geometry (Punegov & Ladanov, 1989*a*).

All the above-mentioned Darwin recurrence relations approaches were obtained for planar structures with atomic planes, which are assumed to be infinitely large in the lateral direction. In recent years there has been a renewed interest in X-ray diffraction on lateral structures (see, *e.g.*, Kaganer & Belov, 2012; Minkevich *et al.*, 2011; Lee *et al.*, 2006 and references therein). Different dynamical diffraction approaches (Olekhnovich & Olekhnovich, 1978; Thorkildsen & Larsen, 1999*b*; Kolosov & Punegov, 2005) using Takagi's equations were employed to calculate rocking curves from ideal (*i.e.* non-deformed) crystals with rectangular cross section. Kinematical diffraction theory was used to simulate X-ray diffraction on deformed crystals having a trapezium cross-sectional shape (Punegov *et al.*, 2006; Punegov & Kolosov, 2007) or an arbitrary cross-sectional shape (Punegov *et al.*, 2007).

However, using Takagi's equations to simulate dynamical X-ray diffraction on lateral crystalline structures (Becker, 1977; Becker & Dunstetter, 1984; Olekhnovich & Olekhnovich, 1980; Saldin, 1982; Chukhovskii *et al.*, 1998; Thorkildsen & Larsen, 1999*a*) is a time-consuming procedure that hinders the use of dynamical diffraction to solve inverse problems for such structures. It is timely to explore possibilities offered by simple algebraic Darwin recurrence relations in application to lateral crystalline structures. This will extend the original one-dimensional Darwin approach to the two-dimensional case in both the Fourier space (reciprocal-space maps, RSMs) and real space (lateral crystalline structures).

The purpose of this paper is to extend Darwin's approach to X-ray dynamical diffraction by lateral crystalline structures. In particular, we demonstrate how our new approach can be used to simulate RSMs for lateral plane-parallel crystalline structures of different sizes and thicknesses.

2. Darwin's diffraction on a plane-parallel crystal

Before proceeding to obtain a new approach to X-ray diffraction by lateral plane-parallel crystalline structures, we provide a short review of Darwin's approach in the case of plane-parallel crystals. Darwin's approach considers a crystal as a combination of atomic planes with a distance d between those planes. Unlike Laue's theory (see, *e.g.*, Authier, 2001), the Darwin model of crystals assumes that all electron density is placed on those atomic planes. The amplitude reflection coefficients, q and $\bar{q}$, and transmission coefficient, $1 - iq_0$, of an atomic plane can be calculated using Fresnel diffraction (Borie, 1967; Yashiro & Takahashi, 2000). On the other hand, these transmission and reflection coefficients are expressible (Chen & Bhattacharya, 1993) in terms of the Fourier coefficients of dielectric susceptibility (polarizability) $\chi_g = -r_0\lambda^2 F_g/(\pi V_c)$, where F_g is the structure factor ($g = 0,\ h,\ \bar{h}$), λ is the wavelength, V_c is the volume of the elementary cell, $r_0 = e^2/(mc^2)$ is the classical electron radius, c is the speed of light in vacuum, and e and m are electron charge and electron mass, respectively.

Thus, the appropriate coefficients in the Darwin recurrence relations can be written as $q_0 = \pi d\chi_0/(\lambda \sin\theta_B)$, $q = \pi d\chi_h/(\lambda \sin\theta_B)$ and $\bar{q} = \pi d\chi_{-h}/(\lambda \sin\theta_B)$, where θ_B is the Bragg angle. In this paper we consider a symmetrical coplanar Bragg diffraction case for σ-polarization. The equations can be extended for π-polarization by incorporating $\cos(2\theta_B)$ into $\chi_{-h,h}$.

Let us consider a plane-parallel crystal having a finite thickness of $L_z = dN$, where N is the number of reflecting atomic planes. The angle between the wavevector of an incident plane wave and the crystal surface is $\theta = \theta_B + \Delta\theta$, where $\Delta\theta$ is a small deviation from the Bragg angle.

Then the transmitted, T_n, and reflected, S_n, wave amplitudes for the nth atomic plane can be written using the following recurrence relations (Darwin, 1914*b*; Authier, 2001):

$$\begin{aligned} T_n &= (1 - iq_0)\exp(i\varphi)T_{n-1} - i\bar{q}\exp(i2\varphi)S_n, \\ S_n &= (1 - iq_0)\exp(i\varphi)S_{n+1} - iqT_n. \end{aligned} \tag{1}$$

Here, T_{n-1}, S_{n+1} are the wave amplitudes for the $(n-1)$th and $(n+1)$th atomic planes, respectively. The additional phase shift, $\varphi = (2\pi d/\lambda)\sin\theta$, is caused by the propagation of the wavefield between the atomic planes. Note that we use a definition of the phase shift without the minus sign (*cf.* Darwin, 1914*b*; Authier, 2001) because we use the following definition for plane waves, $\exp[i(\mathbf{k}\cdot\mathbf{r} - \omega t)]$, instead of $\exp[-i(\mathbf{k}\cdot\mathbf{r} - \omega t)]$ used by other authors. As the angular deviation $\Delta\theta$ is small, the phase shift φ can be written in the following form: $\varphi = (2\pi d/\lambda)(\sin\theta_B + \cos\theta_B\Delta\theta)$. Taking into account the boundary conditions $T_0 = 1$ and $S_N = 0$, the analytical solutions of equation (1) can be presented as follows (Punegov, 1992):

$$\begin{aligned} S_n &= -B\frac{u_2^N u_1^n - u_1^N u_2^n}{(Au_1 - 1)u_2^N - (Au_2 - 1)u_1^N}, \\ T_n &= \frac{(Au_1 - 1)u_2^N u_1^n - (Au_2 - 1)u_1^N u_2^n}{(Au_1 - 1)u_2^N - (Au_2 - 1)u_1^N}, \end{aligned} \tag{2}$$

where $u_{1,2} = \hat{x} \pm (\hat{x}^2 - 1)^{1/2}$,

$$\hat{x} = \frac{1 + (1 - iq_0)^2\exp(i2\varphi) + q\bar{q}\exp(i2\varphi)}{2(1 - iq_0)\exp(i\varphi)},$$

$A = (1 - iq_0)\exp(i\varphi)$ and $B = -iq$. From equation (1) we can get the amplitude reflection, S_0, and transmission coefficient, T_N, of the entire crystal:

$$\begin{aligned} S_0 &= -B\frac{u_2^N - u_1^N}{(Au_1 - 1)u_2^N - (Au_2 - 1)u_1^N}, \\ T_N &= A\frac{u_1 - u_2}{(Au_1 - 1)u_2^N - (Au_2 - 1)u_1^N}. \end{aligned} \tag{3}$$

Taking into account that $u_1^n u_2^n = 1$, equation (3) can be further transformed into

$$S_0 = \frac{-iq}{1-(1-iq_0)\exp(i\varphi)\sin[(N-1)\arccos\hat{x}]/\sin(N\arccos\hat{x})},$$
$$T_N = \frac{(1-iq_0)\exp(i\varphi)(1-\hat{x}^2)^{1/2}}{\sin(N\arccos\hat{x})-(1-iq_0)\exp(i\varphi)\sin[(N-1)\arccos\hat{x}]}. \quad (4)$$

This result is identical to equations (12) and (13) in Perkins & Knight (1984).

Equation (4) can also be rewritten in a more compact form (*cf.* Vardanyan *et al.*, 1985):

$$S_0 = \left(\frac{q}{\bar{q}}\right)^{1/2}\frac{\sin(N\chi)}{\sin(N\chi+\psi)}\exp(-i\varphi),$$
$$T_N = \frac{\sin(\psi)}{\sin(N\chi+\psi)}\exp(-iN\varphi), \quad (5)$$

where

$$\hat{y} = \frac{1-(1-iq_0)^2\exp(i2\varphi)-q\bar{q}\exp(i2\varphi)}{2q\bar{q}\exp(i\varphi)},$$

$\chi = \arccos(\hat{x})$ and $\psi = \arccos(\hat{y})$.

3. Darwin's diffraction on a lateral plane-parallel crystalline structure

Now we use Darwin's methodology of recurrence relations to describe X-ray diffraction on a lateral crystalline structure having width of L_x and thickness of L_z (see Fig. 1). The origin is on a line that is the intersection of two planes, namely the left vertical face and top surface of the structure. The x axis and z axis form a diffraction plane so that the x axis is the intersection of the diffraction plane and the top surface of the structure, and the z axis is the intersection of the diffraction plane and the left vertical face of the structure. Such a shape of the structure is similar, for instance, to the shape of a single quantum wire. We restrict ourselves to the case of a symmetric coplanar Bragg diffraction. The angle between the wavevector of an incident plane wave and the x axis is θ (see Fig. 1).

Let us consider an X-ray beam that goes through the origin. Then this beam travels $d/\sin\theta$ before being reflected by the next atomic plane. The projection of this distance (*i.e.*, $d/\sin\theta$) on the lateral direction is $\Delta x = d\cot\theta$. We can use Δx as a step size along the x axis to indicate the positions $x_m = m\,\Delta x$ (m is an integer) where this beam will be partially transmitted to the next atomic plane or partially reflected.

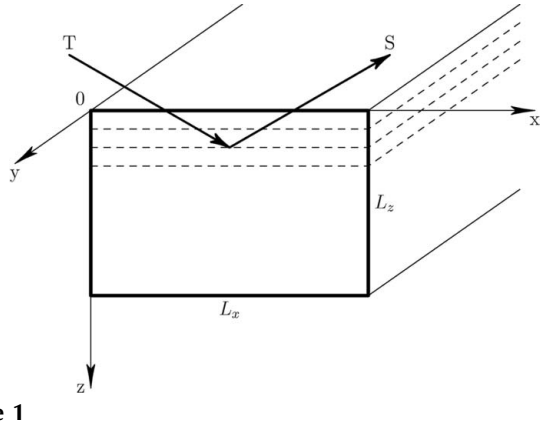

Figure 1
The scheme of Darwin's X-ray diffraction on a lateral crystalline structure with a rectangular cross section.

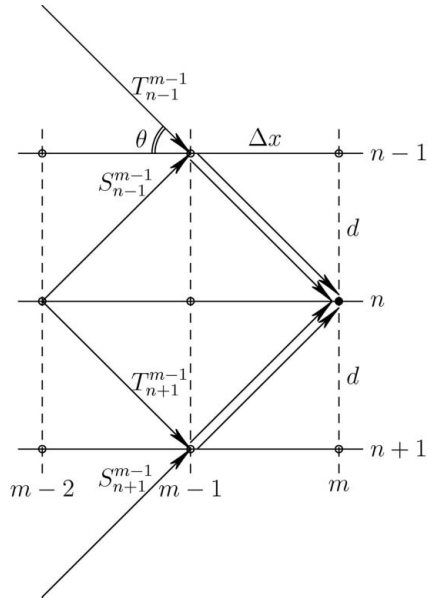

Figure 2
The transmitted, T_i^j, and reflected, S_i^j, waves in the Darwin approach.

Let T_n^m and S_n^m be the amplitudes of the transmitted and reflected waves, respectively, upstream of the $(m; n)$ node of a two-dimensional rectangular lattice. Here, both m and n are integers, where m corresponds to the node's number in the horizontal (lateral) direction, and n in the vertical direction (see Fig. 2). The total number of nodes, $M_x + 1$ and $N_z + 1$, along the x and z axes, respectively, is determined by the structure width, $L_x = M_x\Delta x$, and thickness, $L_z = N_z d$.

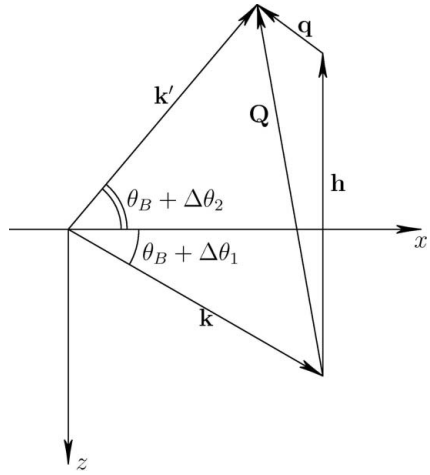

Figure 3
The wavevectors **k**, **k**′ of the incident and reflected waves, respectively. **h** is the vector of the reciprocal lattice. The deviation of the scattering vector, $\mathbf{Q} = \mathbf{k}' - \mathbf{k}$, from the reciprocal-lattice vector **h** is defined by the vector **q**. The angular deviations of **k** and **k**′ from the Bragg angle position are described by $\Delta\theta_1$ and $\Delta\theta_2$, respectively.

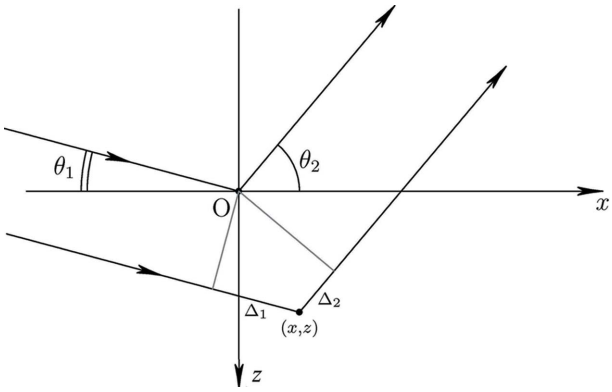

Figure 4
Optical path differences $\Delta_1 = x\cos\theta_1 + z\sin\theta_1$ and $\Delta_2 = -x\cos\theta_2 + z\sin\theta_2$ for an arbitrary point (x, z) in a lateral crystalline structure. Note that the angular deviations are not to scale.

Taking into account dynamical interactions of waves inside the structure, we obtain the following recurrence relations between the reflected, S, and transmitted, T, beams:

$$T_{n+1}^{m} = a\ T_{n}^{m-1} + b_1 S_{n}^{m-1},$$
$$S_{n}^{m} = a\, S_{n+1}^{m-1} + b_2 T_{n+1}^{m-1}, \qquad (6)$$

where $a = (1 - iq_0)\exp(i\varphi_l)$, $b_1 = -i\bar{q}\exp(i\varphi_l)$ and $b_2 = -iq\exp(i\varphi_l)$. It should be noted that in equation (6) we use the expressions for the constants q_0, q and $\bar{q}$ obtained for an infinitely large crystal, which is, obviously, an approximation. Potentially, this method can be extended by way of replacing these three constants by three functions depending on the x and z coordinates. This will allow one to describe local non-homogeneity in the lateral crystalline structures. The phase shift $\varphi_l = (2\pi d)/(\lambda\sin\theta_B)$ is an additional phase shift occurring when the wave propagates from one node to another.

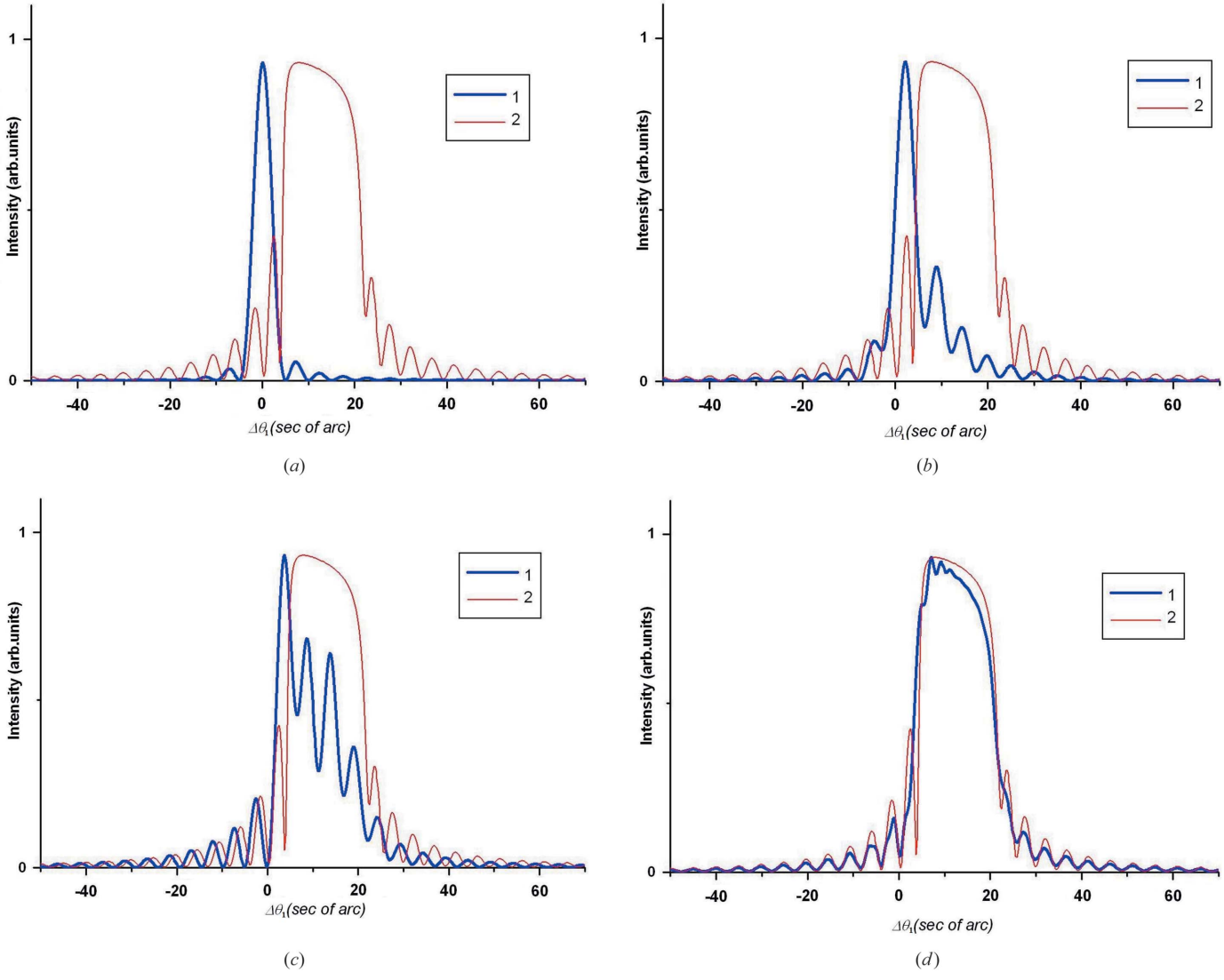

Figure 5
θ–2θ scans (*i.e.* $\Delta\theta_1 = \Delta\theta_2$ or $q_x = 0$) of X-ray diffraction on plane-parallel lateral crystalline structures (thick blue line) with thickness L_z = 3.27 µm for different widths: (*a*) L_x = 1.35 µm, (*b*) L_x = 5.39 µm, (*c*) L_x = 13.5 µm and (*d*) L_x = 53.9 µm. Compare with θ–2θ scans of X-ray diffraction on a plane-parallel crystal (thin red line) with thickness L_z = 3.27 µm and $L_x = \infty$.

Plane-parallel crystals are infinitely large in the lateral direction. Therefore their diffracted intensity distribution shape is a delta-like function depending on the vertical coordinate in Fourier space. Unlike the plane-parallel crystals, the lateral plane-parallel crystalline structures produce a diffracted intensity distribution that has a more complex shape. That is, their diffracted intensity distribution (*i.e.*, RSM) depends on both the vertical and horizontal coordinates in Fourier space.

Let us now assume that the angle between the wavevector $\mathbf{k}$ of the incident plane wave and the x axis is $\theta_1 = \theta_B + \Delta\theta_1$ (see Fig. 3). The reflected wave is registered in the direction of the wavevector $\mathbf{k}'$. The angle between $\mathbf{k}'$ and the x axis is $\theta_2 = \theta_B + \Delta\theta_2$. Both the wavevectors, $\mathbf{k}$ and $\mathbf{k}'$, lie in the diffraction plane and $|\mathbf{k}| = |\mathbf{k}'| = k = 2\pi/\lambda$. We consider the case when the angular deviations $\Delta\theta_1$ and $\Delta\theta_2$ are small. The deviation of the scattering vector $\mathbf{Q} = \mathbf{k}' - \mathbf{k}$ from the reciprocal-lattice vector $\mathbf{h}$ is defined by the vector $\mathbf{q}$ (see Fig. 3). The appropriate projections of the vector $\mathbf{q}$ are

$$q_x = k \sin\theta_B(\Delta\theta_1 - \Delta\theta_2),$$
$$q_z = -k \cos\theta_B(\Delta\theta_1 + \Delta\theta_2). \quad (7)$$

We can also rewrite these relations as $\Delta\theta_{1,2} = \pm(2k\cos\theta_B)^{-1}(q_x \cot\theta_B \mp q_z)$.

Traditionally, the angular deviations of the sample and analyser crystal in the so-called triple-crystal scheme (Iida & Kohra, 1979) are defined by ω and ε, respectively. Then using $\Delta\theta_1 = \omega$ and $\Delta\theta_2 = \varepsilon - \omega$ we can rewrite equation (7) in the following form, which explicitly connects the position in reciprocal space and the experimentally measured angular parameters ω and ε:

$$q_x = k \sin\theta_B(2\omega - \varepsilon),$$

$$q_z = -k \cos\theta_B \varepsilon.$$

The entire phase shift consists of two components: the phase shift of the transmitted wave and the phase shift of the reflected wave. These additional phase shifts are defined *via* optical path differences. We choose the origin (see Figs. 1 and 4) as a reference point in our calculation of the additional phase shits. For X-rays incident on the left vertical face of the structure ($x = 0$) the optical path difference increases along the z direction as $z \sin\theta_1$ (see Fig. 4). The phase shift at the node positions $z_n = nd$ along the z direction is $\varphi^n_{z,\text{in}} = (2\pi/\lambda)nd \sin\theta_1$. Thus the boundary conditions at the left face of the structure ($x = 0$) are $T^0_n = \exp(i\varphi^n_{z,\text{in}})$ and $S^0_n = 0$, where $n = 0, 1, 2, \ldots, N_z - 1$.

For X-rays incident on the top surface of the structure ($z = 0$) the optical path difference increases along the x direction as $m\Delta x \cos\theta_1$. Therefore, the phase shift of the incident wave in both the lateral and vertical directions depends on θ_1. The appropriate boundary condition at the top surface of the structure can be written as $T^m_0 = \exp(i\varphi^m_{x,\text{in}})$, where $\varphi^m_{x,\text{in}} = (2\pi/\lambda)m\Delta x \cos\theta_1$ and $m = 1, 2, \ldots, M_x$.

Considering that the exiting X-ray wave emerges from the top surface and the right vertical face of the structure (see Fig. 1), the boundary conditions for the reflected wave S at the bottom surface and the left vertical face of the structure are $S^m_{N_z} = 0$ and $S^0_n = 0$, respectively.

In accordance with the model (see Fig. 2), we use a rectangular $M_x \times N_z$ lattice having a fixed distance between nodes to describe the dynamical diffraction process.

The simulation procedure based on equation (6) consists of the external and internal cycles. The external cycle (from left to right) starts with the first column ($m = 1$) and goes up to the last column ($m = M_x$). Note that the left vertical face of the structure corresponds to the 0th column. The internal cycle (from top to bottom) starts with the first reflecting plane ($n = 1$) and goes up to the last one ($n = N_z$). Note that the top surface of the structure corresponds to the 0th plane. For instance, for the first column we use the external boundary conditions to calculate amplitudes of the reflected and transmitted waves at each node of the column $\{S^1_n\} = (S^1_0, S^1_1, S^1_2, \ldots, S^1_{N_z-1})$ and $\{T^1_n\} = (T^1_1, T^1_2, T^1_3, \ldots, T^1_{N_z})$, respectively. Then substituting the amplitudes calculated for the first column in equation (6) we can calculate the amplitudes for the second column, namely $\{S^2_n\}$ and $\{T^2_n\}$, and so on. At the end of the external cycle we obtain arrays of the reflected and transmitted amplitudes, namely $\{S^m_n\}$ and $\{T^m_n\}$, at each node of the two-dimensional lattice. Note that according to the boundary conditions we apply for the amplitudes the following phase factors: $\exp(i\varphi^n_{x,\text{in}})$, where $\varphi^m_{x,\text{in}} = (2\pi/\lambda)m\Delta x \cos\theta_1$, when we do calculations for the mth column, and $\exp(i\varphi^n_{z,\text{in}})$, where $\varphi^n_{z,\text{in}} = (2\pi/\lambda)nd \sin\theta_1$, when we do calculations for the nth plane.

Hence, using equation (6) and the boundary conditions for the entering wavefield we are able to calculate the reflection amplitudes, $\{S^m_n(\theta_1)\}$, at each node. To calculate the entire reflection amplitude we have to take into account the additional phase shifts, defined by the direction of the vector $\mathbf{k}'$ or the angle θ_2.

The amplitude reflection coefficient, $S(\theta_1, \theta_2)$, of the lateral plane-parallel crystalline structure is a sum of the amplitudes of waves exiting the top surface of the structure, namely $\{S^m_0(\theta_1)\}$, and the right vertical face of the structure, namely $\{S^{M_x}_n(\theta_1)\}$, with additional phase factors:

$$S(\theta_1, \theta_2) = \sum_{m=0}^{M_x} S^m_0(\theta_1) \exp(i\varphi^m_{x,\text{ex}}) + \sum_{n=1}^{N_z} S^{M_x}_n(\theta_1) \exp(i\varphi^n_{z,\text{ex}}) \exp(i\varphi^{M_x}_{x,\text{ex}}), \quad (8)$$

where the additional phase factors $\varphi^m_{x,\text{ex}} = -(2\pi/\lambda)m\Delta x \cos\theta_2$ and $\varphi^n_{z,\text{ex}} = (2\pi/\lambda)nd \sin\theta_2$ depend on $\theta_2 = \theta_B + \Delta\theta_2$. The phase factor $\exp(i\varphi^{M_x}_{x,\text{ex}})$ takes into account the x coordinate of the right vertical face of the structure, namely $L_x = M_x\Delta x$.

Thus, the amplitude $S(\theta_1, \theta_2)$ depends on both θ_1 and θ_2. Therefore equation (8) allows one to simulate RSMs. Also one can use equation (8) to calculate the appropriate directional scans in reciprocal space. For instance, a q_z-scan (CTR) simulation can be done if $\theta_1 = \theta_2$ (or $2\omega = \varepsilon$).

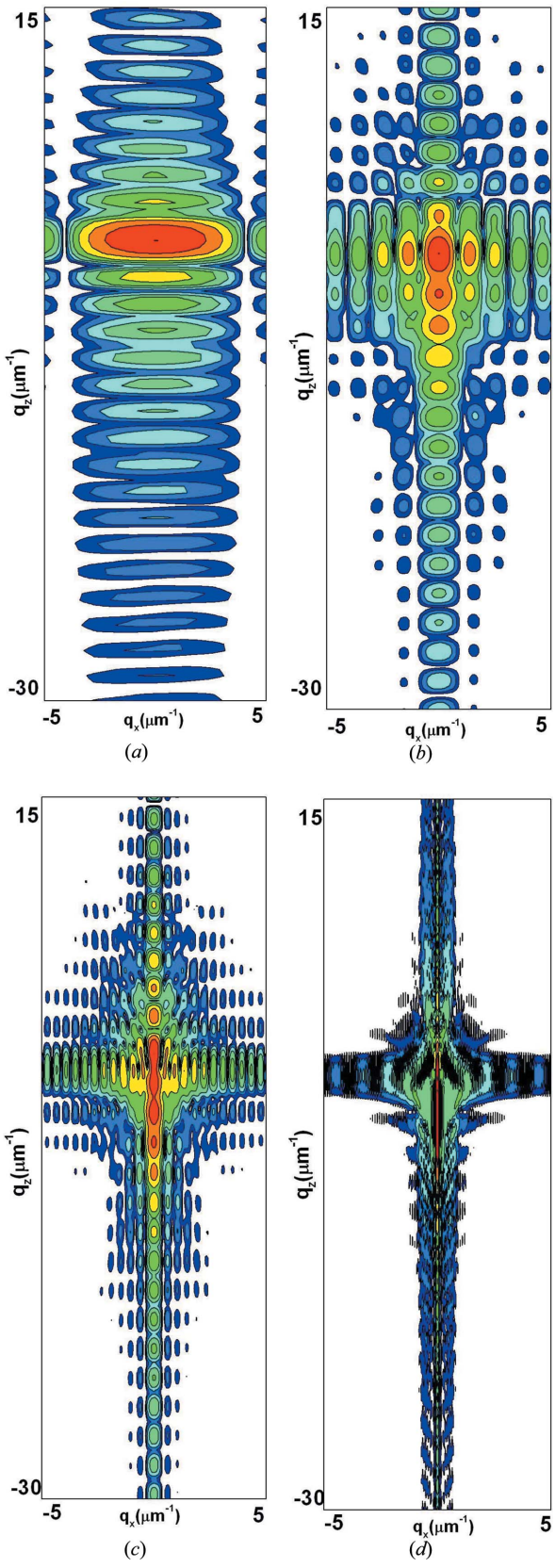

Figure 6
RSMs of X-ray diffraction on plane-parallel lateral crystalline structures with thickness L_z = 3.27 μm and different widths: (*a*) L_x = 1.35 μm, (*b*) L_x = 5.39 μm, (*c*) L_x = 13.5 μm and (*d*) L_x = 53.9 μm.

4. Numerical modelling

The numerical modelling of RSMs and directional scans in reciprocal space is performed using equations (6) and (8). In our simulations we use Cu $K\alpha_1$ radiation (the wavelength is 0.154056 nm) for the (111) reflection of a Ge lateral crystalline structure. The thickness of this structure is $L_z = 10000\, d_{111} =$ 3.27 μm. We use several widths of the structure: L_x = 1.35, 5.39, 13.5, 53.9 μm, which correspond to the following number of nodes M_x = 1000, 4000, 10000, 40000, respectively. In an effort to carry out a proper normalization all simulated reflected wave intensities were normalized on the maximum intensity of the Darwin curve for a plane-parallel crystal of the same thickness.

Rocking curves shown in Fig. 5 were simulated using equation (8) for the case of ω–2θ scans (*i.e.* $\theta_1 = \theta_2$). Then the optical path difference $\Delta = \Delta_1 + \Delta_2 = 2z \sin\theta$ ($\theta = \theta_1 = \theta_2$) (see Fig. 4) does not depend on the x coordinate, and the entire phase shift at the top surface of the structure is $\varphi_x^m = \varphi_{x,\mathrm{in}}^m + \varphi_{x,\mathrm{ex}}^m = 0$.

The extinction length (Authier, 2001) for the Ge(111) reflection for a semi-infinite crystal is 0.67 μm, the full width at half-maximum (FWHM) of the Darwin curve is 15.4 arcsec (Stepanov & Forrest, 2008). In the case of small lateral width (L_x = 1.35 μm) the simulated rocking curve corresponds to the kinematical limit (see Fig. 5*a*). As the width of the structure increases we observe a gradual transfer into dynamical diffraction (see Figs. 5*b*, 5*c*), where thickness oscillations are still observable even within the angular region of Darwin's 'table'. For a large width of the structure (L_x = 53.9 μm) the simulated rocking curves for a lateral crystalline structure and a plane-parallel crystal are in close agreement (see Fig. 5*d*).

Fig. 6 shows the RSM simulations for lateral crystalline structures of different width. If the lateral width is small, the shape of the RSM (see Fig. 6*a*) is consistent with a typical kinematical diffraction case (Authier, 2001):

$$I(q_x, q_z) = \left|S(q_x, q_z)\right|^2 \propto \left|\mathrm{sinc}(q_x L_x/2)\right|^2 \left|\mathrm{sinc}(q_z L_z/2)\right|^2,$$

where $\mathrm{sinc}(x) = \sin(x)/x$. Both the width of the central peak and the period of lateral oscillations in the q_x direction decrease as the lateral width of the structure increases. The period of lateral oscillations is inversely proportional to the lateral size of the structure as evident from Fig. 7, which shows q_x-scans across the central peak of the RSM.

The obtained simulation results are in good agreement with the solution obtained by integration of Takagi's equations (Kolosov & Punegov, 2005).

5. Conclusion

We demonstrated that Darwin's approach using algebraic recurrence relations can be extended to the case of lateral plane-parallel crystalline structures. This approach, being simple and transparent, is faster than the one based on Takagi's equations and allows simulations of RSMs. It is especially important for the solution of inverse problems using minimization of the discrepancy between experimental and

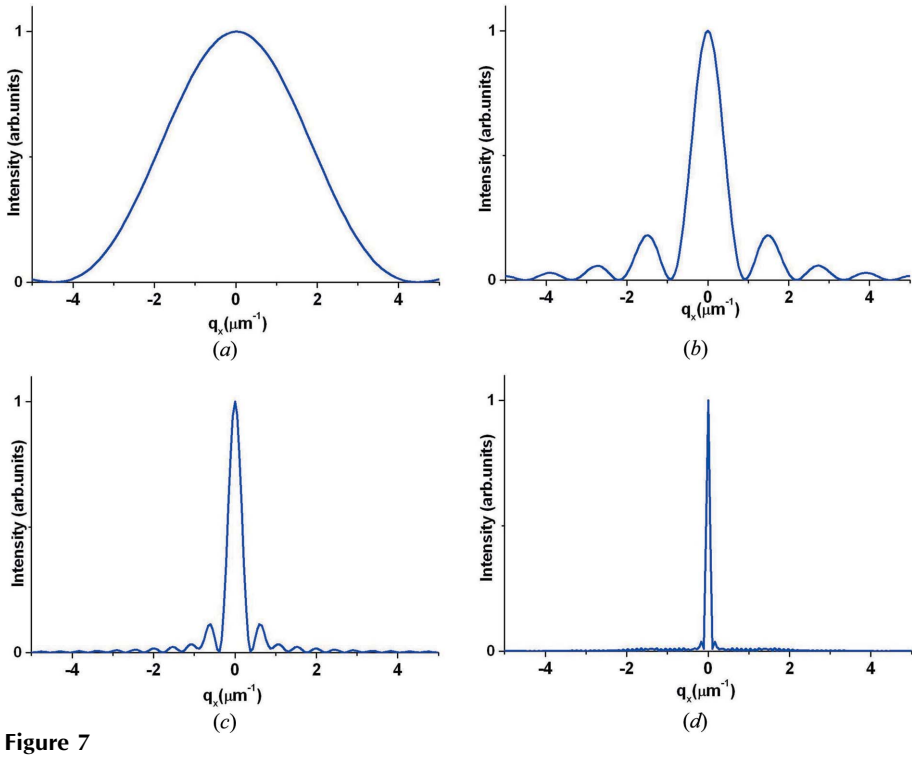

Figure 7
q_x scans (across the central peak of the RSM) of X-ray diffraction on plane-parallel lateral crystalline structures with thickness L_z = 3.27 μm and different widths: (*a*) L_x = 1.35 μm, (*b*) L_x = 5.39 μm, (*c*) L_x = 13.5 μm and (*d*) L_x = 53.9 μm.

simulated data (Pavlov *et al.*, 1995; Kirste *et al.*, 2005). Therefore this new approach can be widely used for non-destructive testing of lateral structures used in opto- and microelectronics devices, nonvolatile memory devices and X-ray optics. This approach can potentially be extended further to the three-dimensional case in both the Fourier space and real space.

This study was supported in part by the Russian Foundation for Basic Research (project No. 13-02-00272-a), the Presidium of the Russian Academy of Sciences (project No. 12-P-1-1014) and the Ural Branch of the Russian Academy of Sciences (basic research program project No. 12-U-1–1010). KMP acknowledges financial support from the University of New England.

References

Abramowitz, M. & Stegun, I. A. (1972). Editors. *Handbook of Mathematical Functions with Formulas, Graphs, and Mathematical Tables.* New York: Dover Publications.
Authier, A. (2001). *Dynamical Theory of X-ray Diffraction.* Oxford University Press.
Bartels, W. J., Hornstra, J. & Lobeek, D. J. W. (1986). *Acta Cryst.* A**42**, 539–545.
Becker, P. (1977). *Acta Cryst.* A**33**, 243–249.
Becker, P. & Dunstetter, F. (1984). *Acta Cryst.* A**40**, 241–251.
Belyaev, Y. N. & Kolpakov, A. V. (1983). *Phys. Status Solidi*, **76**, 641–646.
Bezirganian, P. H. & Navasardian, M. A. (1969). *Izv. Akad. Nauk Arm. SSR Fiz.* **3**, 269–274.
Borie, B. (1966). *Acta Cryst.* **21**, 470–472.
Borie, B. (1967). *Acta Cryst.* **23**, 210–216.
Bushuev, V. A. (1989). *Sov. Phys. Solid State*, **31**, 1877–1882.
Caticha, A. (1994). *Phys. Rev. B*, **49**, 33–38.
Chandrasekhar, S. & Rao, K. N. S. (1968). *Acta Cryst.* A**24**, 445–451.
Chen, Y. C. & Bhattacharya, P. K. (1993). *J. Appl. Phys.* **73**, 7389–7394.
Chukhovskii, F. N., Hupe, A., Rossmanith, E. & Schmidt, H. (1998). *Acta Cryst.* A**54**, 191–198.
Chung, J.-S. & Durbin, S. M. (1999). *Acta Cryst.* A**55**, 14–19.
Darwin, C. G. (1914*a*). *Philos. Mag.* **27**, 315–333.
Darwin, C. G. (1914*b*). *Philos. Mag.* **27**, 675–691.
Dub, P. & Litzman, O. (1999). *Acta Cryst.* A**55**, 613–620.
Durbin, S. M. (1995). *Acta Cryst.* A**51**, 258–268.
Durbin, S. & Follis, G. (1995). *Phys. Rev. B*, **51**, 10127–10133.
Fitzgerald, W. J. & Darlington, C. N. W. (1976). *Acta Cryst.* A**32**, 671–672.
Ignatovich, V. K. (1990). *Sov. Phys. JETP*, **70**, 913–917.
Ignatovich, V. K. (1992). *Sov. Phys. Crystallogr.* **37**, 588–595.
Iida, A. & Kohra, K. (1979). *Phys. Status Solidi*, **51**, 533–542.
Kaganer, V. M. & Belov, A. Y. (2012). *Phys. Rev. B*, **85**, 125402.
Kirste, L., Pavlov, K. M., Mudie, S. T., Punegov, V. I. & Herres, N. (2005). *J. Appl. Cryst.* **38**, 183–192.
Kolosov, S. I. & Punegov, V. I. (2005). *Crystallogr. Rep.* **50**, 357–362.
Kolpakov, A. V. & Punegov, V. I. (1985). *Solid State Commun.* **54**, 573–578.
Kuznetsov, A. V. & Fofanov, A. D. (1970). *Sov. Phys. J.* **13**, 1269–1274.
Kuznetsov, A. V. & Fofanov, A. D. (1972). *Sov. Phys. J.* **15**, 559–563.
Ladanov, A. V. & Punegov, V. I. (1989). Twelfth European Crystallographic Meeting, Moscow, USSR, August 20–29, 1989. Collected Abstracts Vol. 3, p. 137.
Lee, K., Yi, H., Park, W., Kim, Y. K. & Baik, S. (2006). *J. Appl. Phys.* **100**, 051615.
Li, M., Ress, H., Gerhard, T., Landwehr, G., Cui, S. F. & Mai, Z. H. (1997). *J. Appl. Phys.* **81**, 2143–2147.
Minkevich, A. A., Fohtung, E., Slobodskyy, T., Riotte, M., Grigoriev, D., Metzger, T., Irvine, A. C., Novák, V., Holý, V. & Baumbach, T. (2011). *EPL*, **94**, 66001.
Nakatani, S. & Takahashi, T. (1994). *Surf. Sci.* **311**, 433–439.
Olekhnovich, N. M. & Olekhnovich, A. I. (1978). *Acta Cryst.* A**34**, 321–326.
Olekhnovich, N. M. & Olekhnovich, A. I. (1980). *Acta Cryst.* A**36**, 22–27.
Pavlov, K. M. & Punegov, V. I. (1998). *Acta Cryst.* A**54**, 214–218.
Pavlov, K. M. & Punegov, V. I. (2000). *Acta Cryst.* A**56**, 227–234.
Pavlov, K. M., Punegov, V. I. & Faleev, N. N. (1995). *J. Exp. Theor. Phys.* **80**, 1090–1097.
Perkins, R. T. & Knight, L. V. (1984). *Acta Cryst.* A**40**, 617–619.
Pietsch, U., Holý, V. & Baumbach, T. (2004). *High Resolution X-ray Scattering: From Thin Films to Lateral Nanostructures*, 2nd ed. New York: Springer-Verlag.
Prins, J. A. (1930). *Z. Phys.* **63**, 477–493.
Prudnikov, I. R. (1998). *Acta Cryst.* A**54**, 1034–1036.
Prudnikov, I. R. (2000). *Phys. Status Solidi*, **217**, 725–735.
Punegov, V. I. (1990). *Sov. Phys. Crystallogr.* **35**, 336–340.
Punegov, V. I. (1991). *Sov. Phys. Solid. State*, **33**, 136–140.
Punegov, V. I. (1992). *Sov. Tech. Phys. Lett.* **18**, 120–122.

Punegov, V. I. (1993). *Phys. Status Solidi*, **136**, 9–19.
Punegov, V. I. & Kolosov, S. I. (2007). *Crystallogr. Rep.* **52**, 191–198.
Punegov, V. I., Kolosov, S. I. & Pavlov, K. M. (2006). *Tech. Phys. Lett.* **32**, 809–812.
Punegov, V. I. & Ladanov, A. V. (1989*a*). *Sov. Phys. Tech. Phys.* **34**, 1351–1352.
Punegov, V. I. & Ladanov, A. V. (1989*b*). Twelfth European Crystallographic Meeting, Moscow, USSR. August 20–29, 1989. Collected Abstracts Vol. 3, p. 93.
Punegov, V. I. & Ladanov, A. V. (1990). *Poverkhnost*, **4**, 45–50.
Punegov, V. I., Maksimov, A. I., Kolosov, S. I. & Pavlov, K. M. (2007). *Tech. Phys. Lett.* **33**, 125–127.
Punegov, V. I. & Vishnjakov, Y. V. (1995). *J. Phys. D Appl. Phys.* **28**, A184–A188.
Robinson, I. K. (1986). *Phys. Rev. B*, **33**, 3830–3836.
Saldin, D. K. (1982). *Acta Cryst.* A**38**, 425–432.
Stepanov, S. & Forrest, R. (2008). *J. Appl. Cryst.* **41**, 958–962.
Takagi, S. (1962). *Acta Cryst.* **15**, 1311–1312.
Takahashi, T. & Nakatani, S. (1995). *Surf. Sci.* **326**, 347–360.
Takahashi, T., Yashiro, W., Takahasi, M., Kusano, S., Zhang, X. & Ando, M. (2000). *Phys. Rev. B*, **62**, 3630–3638.
Thorkildsen, G. & Larsen, H. B. (1999*a*). *Acta Cryst.* A**55**, 1–13.
Thorkildsen, G. & Larsen, H. B. (1999*b*). *Acta Cryst.* A**55**, 840–854.
Vardanyan, D. M., Manoukyan, H. M. & Petrosyan, H. M. (1985). *Acta Cryst.* A**41**, 212–217.
Yashiro, W., Ito, Y., Takahasi, M. & Takahashi, T. (2001). *Surf. Sci.* **490**, 394–408.
Yashiro, W. & Takahashi, T. (2000). *Acta Cryst.* A**56**, 163–167.